^{1}H NMR AND MOLECULAR MODELING STUDIES OF SULFONAMIDE/β-CYCLODEXTRIN INCLUSION COMPLEXES

Philip E. Pfeffer, Gregory King, Peter L. Irwin, Jeffrey D. Brewster

U.S. Department of Agriculture, Agricultural Research Service, Eastern Regional Research Center, Wyndmoor, Pennsylvania, USA

^{1}H NMR spectroscopy studies yielded the conformations and association constants of four sulfonamide/β-cyclodextrin inclusion complexes. Relative association free energies were calculated using a thermodynamic cycle in which non-covalent association or dissociation reactions were separated into a sum of reactions involving only changes to electrostatic or hydrophobic variables. Two sets of calculations were performed: one in which the model systems include solvent, and the other in which the model systems do not include solvent. The calculations are accurate to roughly ± 1.5 kcal/mol. The solvated model is better than the unsolvated one based upon linear least-squares fits of the calculated results to the experimental values. The calculations performed with the solvated model correctly select the preferred binding conformation based on the NMR data (two distinct conformations exist for each of the complexes considered here) in three out of the four cases examined. Contributions to the calculated association free energies from electrostatic interactions indicate that the formation of these inclusion complexes is not driven solely by the hydrophobic effect. J Magn Reson Anal 1997; 3:99-107.

The complexes formed by inclusion of guest species within the cavities of cyclodextrins (CDs) (also known as cyclomalto-oligosaccharides, which are cyclic polymers composed of 6 to 8 α-glucopyranose monomers connected by α–1,4 linkages) can be utilized in a variety of applications (1). Many of these applications take advantage of the fact that the cavities of cyclodextrins provide an attractive microenvironment for hydrophobic species. For instance CDs have been enlisted to carry insecticides that are only weakly soluble in water to their destinations (2). In addition β-linked cyclic glucans have also been implicated as carriers of hydrophobic signal compounds in symbiotic plant/microbe systems (3).

Reprint address: P. E. Pfeffer, U.S. Department of Agriculture, Agricultural Research Service, Eastern Regional Research Center, 600 East Mermaid Lane, Wyndmoor, PA 19038
Telephone (215) 233-6469, Fax (215) 233-6581

Current analytical methods for the detection of sulfonamides (sulfa drugs) residues in food require the use of organic solvents such as methanol, chloroform, acetone, n-hexane, methylene chloride, and diethyl ether in extraction and chromatographic procedures. The size and shape of the sulfonamides molecules with the generic formula RSO_2NHR', where R is an aniline ring attached at the four position to S, and R' is typically another ring moiety (*Fig. 1*) suggest the possibility of a new method in which CDs would act as extraction agents for sulfonamides in an aqueous medium. Such a method would eliminate or greatly reduce the need for organic solvents in this application.

It is known that sulfonamides do in fact form inclusion complexes with βCD (the heptamer). The association constants of several of these complexes have been measured (4, 5), and fall in the range 140-1860 at 25°C. However, βCD also bind a variety of other molecules of approximately the same size as the sulfonamides, with association constants in this same

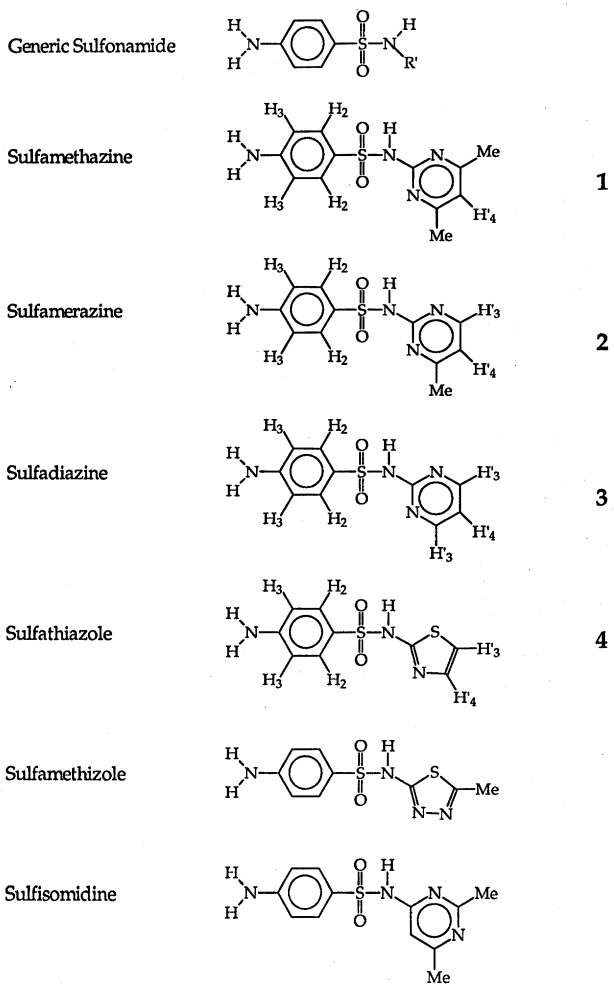

FIGURE 1. Schematic structures of a generic sulfonamide molecule and the six specific sulfonamides examined in our computational study. The four sulfonamides examined in our ^1H NMR study are labeled 1, 2, 3, and 4. The non-exchanging protons of these four structures have been labeled for reference to the NMR resonances (see Table II).

range. A preference for binding to sulfonamides could possibly be achieved by appropriately modifying βCD synthetically. Such a modification would also improve the sensitivity of this method so that lower concentrations of sulfonamides could be detected.

Many laboratories that develop new compounds intended to possess specific target properties (*e.g.* pharmaceuticals) are now avoiding much of the costly trial-and-error syntheses of candidate compounds by using molecular modeling in their projects' initial stages. The results of molecular modeling can often be used to establish which of a list of candidate compounds are likely to be effective for a given purpose, so that only the most promising candidates need to be synthesized and tested in the laboratory.

Here we use NMR spectroscopy in conjunction with molecular modeling with the eventual goal of developing a synthetically-modified CD that will bind to sulfonamides with greater strength and specificity than the unmodified CD. ^1H NMR studies of four of the six sulfonamide/βCD inclusion complexes were performed in order to determine the actual conformations of the complexes, since the previous work (4, 5) did not provide information at this level of detail. The NMR studies also yielded the association constants and stoichiometries of the complexes, establishing a three-way consistency check among the calculations, the current experimental results, and the previous experimental results.

Two independent sets of calculations were performed: one in which the model system included water (Method 1), and the other in which the model system did not include water (Method 2). In Method 1, all dielectric effects are assumed to be represented adequately by the water molecules present in the system (*i.e.* electrostatic interactions are calculated using a dielectric constant of unity). In Method 2, the dielectric effects of the missing water are accounted for empirically by employing a distance-dependent dielectric function in the calculation of electrostatic interactions. Method 1 has the advantage of representing the actual system more faithfully than Method 2. However, due to the larger number of atoms included, computer simulations of the solvated model are much more time-consuming than simulations of the unsolvated one.

Before attempting to predict the sulfonamide-binding properties of particular CD derivatives, we must first establish the reliability of the computational method being used. For this purpose, we chose to calculate the association free energies of six sulfonamide/βCD inclusion complexes, and compare the calculated results to those obtained from experiments.

A thermodynamic cycle was used in both Methods 1 and 2 (see Experimental section) which yields the relative (as opposed to standard) association free energies of the sulfonamide/βCD complexes. The reliability of the two methods may be assessed by comparing these relative association free energies to the standard free energies obtained from experiments (allowing for experimental and calculated values to differ by a constant).

The βCD cavity is large enough to hold only one of the two rings of a given sulfonamide molecule, thus making it necessary to consider both of the possible binding conformations. In the first conformation, the aniline ring (R) is inserted in the βCD cavity, and the variable ring (R') is exposed to solvent. In the second conformation, the roles of the two rings are reversed. Since one of the two conformations is in most cases probably preferred energetically over the other, another test of the method is whether the calculations correctly select the preferred conformation of each complex.

EXPERIMENTAL METHODS

NMR Spectroscopy

^{1}H NMR spectra were obtained with a JEOL GX-400 NMR spectrometer (6). The sulfonamide and βCD mixtures were examined in D_2O containing 20 mM phosphate buffer at pH 7.0. The initial sulfonamide concentrations were in the range of 0.5 - 1×10^{-3} M. The ratio of βCD/sulfonamide varied from 12:1 to 0.168:1. Partial suppression of the HDO peak was accomplished by presaturation. All peaks were referenced to HDO at 4.75 ppm (25°C).

Each spectrum was obtained with 128 scans, 3000 Hz sweep width, 32K data points, 10 msec (90°) pulse, a 5 sec repetition time, and 0.2 Hz exponential line broadening. Linewidths were measured as full widths at half heights. Homogeneity of samples was checked with the linewidth of internal standard p-dioxane.

T_2 measurements were made using the Carr-Purcell-Meiboom-Gill modification (7). Each spectrum required 32 scans, a pulse repetition rate of 45 sec, 9.3 msec 90° pulse, 2t = 4 msec and a spectral width of 650 Hz.

Stoichiometry of the sulfadiazine/βCD complex was determined using Job's method of continuous variation (8). In this procedure, the sum of the initial concentration of sulfadiazine, $[X]_0$, and the initial concentration of βCD, $[Y]_0$, was held at 1.8 mM (*i.e.* $[X]_0+[Y]_0 = 1.8$ mM). The individual concentrations $[X]_0$ and $[Y]_0$ were varied to yield mole fractions of 0.1 to 0.9 in increments of 0.1. To construct a Job plot, the quantity $\Delta\delta_X[X]_0$ or $\Delta\delta_Y[Y]_0$ is plotted against the mole fractions c_X or c_Y, respectively. Here $\Delta\delta_X$ is the chemical shift of X in a solution containing X + Y relative to the chemical shift of X in a solution containing only X. $\Delta\delta_Y$ is defined similarly. The ratio of the mole fractions at which the maxima of the two curves occur determines the stoichiometries of the complexes.

Assuming a one-to-one binding stoichiometry for the complexes, the association constants are:

$$K_a = \frac{[XY]}{[X][Y]} \qquad [1]$$

where [X], [Y], and [XY] are the equilibrium concentrations of sulfonamide, βCD, and sulfonamide/βCD complex, respectively. Expressing [X] and [Y] in terms of the initial concentrations $[X]_0$ and $[Y]_0$, we have:

$$K_a = \frac{[XY]}{([X]_0-[XY])([Y]_0-[XY]} \qquad [2]$$

Recognizing that $\Delta\beta_X$ may be expressed as:

$$\Delta\delta_X = \frac{\Delta\delta_{X,\max}[XY]}{[X_0]} \qquad [3]$$

where $\Delta\delta_{X,max}$ is the value of $\Delta\delta_X$ in the limit of $[Y]\rightarrow\infty$, Eq. 3 may be expressed as K_a =

$$\frac{[X]_0\Delta\delta_X/\Delta\delta_{X,\max}}{\left([X]_0-[X]_0\Delta\delta_X\right)/\Delta\delta_{X,\max}\left([Y]_0-[X]_0\Delta\delta_X/\Delta\delta_{X,\max}\right)} \qquad [4]$$

Solving Eq. 4 for $\Delta\delta_X$ yields:

$$\Delta\delta_X = \frac{\Delta\partial_{x,\max}\left(C-\left[C^2-4K_a^2[X]_0[Y]_0\right]^{1/2}\right)}{2K_a[X_0]} \qquad [5]$$

where $C = 1+K_a([X]_0+[Y]_0)$. The unknowns $\Delta\delta_{X,max}$ and K_a were evaluated by fitting the experimental $\Delta\delta_X$ values to the above equation utilizing a modified Gauss-Newton computer spreadsheet.

Calculations

The sulfonamide and βCD molecules used in this study were "built" using Tripos Associates' SYBYL software package (6). Residual charges were assigned to the βCD atoms using the electronegativity equalization algorithm of Gasteiger and Marsili (9), and to the sulfonamide atoms using a linear combination of Gasteiger-Marsili charges and charges obtained from MNDO (10) calculations (these two methods of assigning charges are available as part of the SYBYL package). SYBYL was also used to build the sulfonamide/βCD complexes. We did not attempt to find the global energy minima of the complexes, since these configurations would not have been retained in the subsequent MD simulations.

The SCAAS model (11) (with several new features) was employed in all of the free energy calculations, using the atomic charge parameters as described above, and the standard SYBYL force field (12) for bonded and van der Waals interactions. A cutoff of 8 Å was used for all nonbonded interactions. The nonbonded interaction lists were based on electrically-neutral groups of atoms (this prevents spurious charges from being created by the application of the cutoff). A time step of 2.0 fsec was used in propagating the MD simulations, with gentle velocity scaling applied to keep the system temperature near the specified value.

In the SCAAS model the solute molecule(s) is/are immersed within a spherical droplet of solvent molecules (water, in this case). For Method 1 calculations the radii of the solvent spheres were set to the radial distance of the solute atom farthest from the origin plus 6 Å. For Method 2 calculations no solvent was included.

Electrostatic interactions between atoms i and j, are calculated as $332q_iq_j/e_{ij}r_{ij}$, where q_i and q_j are the atomic charges (in atomic units), r_{ij} is the distance between the two atoms (in Å), e_{ij} is the dielectric function, and the factor 332 is included to make energies come out in kcal/mol. In Method 1, a dielectric constant of unity was used, while in Method 2 a dielectric function $1+r_{ij}$ was used to empirically compensate for the missing solvent. Except for the difference in dielectric functions, the Method 1 and Method 2 force fields were the same.

In the solvated model (Method 1), the solvent molecules are subjected to a radial constraint that maintains the proper solvent density and prevents evaporation. There is also an important polarization constraint (11) that controls the orientation of the solvent dipole moment vectors near the surface of the system. This constraint counteracts the effect of the presence of the solvent-vacuum interface, which would otherwise cause solvent molecules near the surface to adopt orientations different from those expected in an actual system.

In both Methods 1 and 2, relative association free energies were calculated using the thermodynamic cycle devised by Honig and coworkers (13) (illustrated in *Fig. 2*) in which association or dissociation reactions are separated into a series of four reactions involving changes in either purely electrostatic or purely hydrophobic properties of the system. In this cycle, the association reaction *X(aq) + Y(aq) (XY(aq)* is decomposed into the following four steps:

Step 1	$X(aq) \rightarrow X'(aq)$	$-\Delta G_{elec}(X)$
Step 2	$Y(aq) \rightarrow Y'(aq)$	$-\Delta G_{elec}(Y)$
Step 3	$X'(aq)+Y'(aq) \rightarrow X'Y'(aq)$	$\gamma\left(S_{X'Y'}-S_{X'}-S_{Y'}\right)$
Step 4	$X'Y'(aq) \rightarrow XY(aq)$	$\Delta G_{elec}(XY)$
	$X(aq)+Y(aq) \rightarrow XY(aq)$	ΔG_{assoc}

$$\Delta G_{assoc} = -\Delta G_{elec}(X)-\Delta G_{elec}(Y)+\gamma\left(S_{X'Y'}-S_{X'}-S_{Y'}\right)+\Delta G_{elec}(XY) \quad [6]$$

where X represents a sulfonamide, Y is βCD and XY is the complex.

In Step 1, the residual atomic charges of a single X molecule isolated from other solute species are all gradually turned off to produce X'. In Step 2, a single Y molecule is similarly discharged in the absence of any other solute species to yield Y'.

In Step 3, the chargeless entities X' and Y' are brought together to form the complex X'Y'. There are two contributions to the change in free energy connected with this reaction. The first contribution, $\Delta G_{hphobic}$, is due to the so-called hydrophobic effect. The hydrophobic effect is used to describe phenomena caused by the disruption of water's hydrogen bonding network that occurs when nonpolar solutes are solvated. The number of hydrogen bonds affected by the insertion of a nonpolar solute into water is proportional to the water-accessible surface area of the solute, and thus the free energy penalty for the disruption of the hydrogen bonding network is proportional to this surface area. $\Delta G_{hphobic}$ is thus proportional to the change in solvent-accessible surface area that occurs when isolated X' and Y' molecules are brought together to form the complex X'Y'. $\Delta G_{hphobic}$ is calculated empirically as $\Delta G_{hphobic} = \gamma(S_{X'Y'} - S_{X'} - S_{Y'})$, where a microscopic surface tension $\gamma = 0.05$ kcal mol^{-1}Å^{-2} is used (13), and S_A is the solvent-accessible surface area of solute species A.

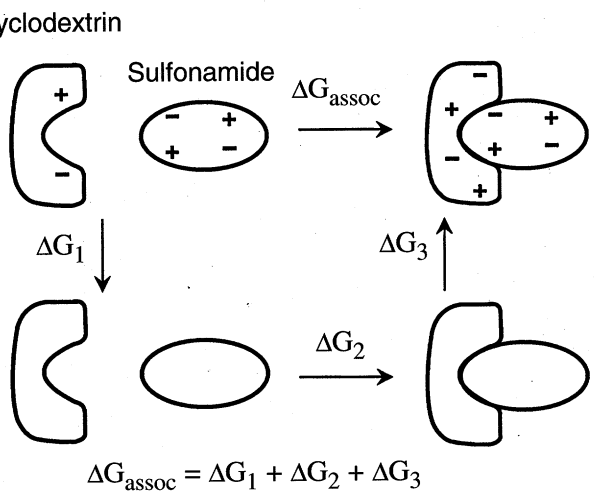

FIGURE 2. The thermodynamic cycle employed in the calculation of association free energies. In the first stage of the cycle (ΔG_1), the atomic charges of the reactants (which are simulated separately, and are thus much farther apart than is indicated in the figure) are removed. In the second stage (ΔG_2), the discharged (hydrophobic) reactants are brought together to form a complex. In the third stage (ΔG_3), the original atomic charges are restored. The free energy differences for the first and third stages involve only changes in electrostatic variables, and the free energy difference for the second stage involves only the change in the solvent-accessible surface area of the solutes that occurs upon complexation.

The other contribution to the free energy difference in Step 3 is due to changes in van der Waals interactions. Upon complexation, some of the solute-water van der Waals interactions are replaced by solute-solute and water-water van der Waals interactions. The total number of interactions remains roughly the same, however, and since deviations in the magnitudes of van der Waals interaction energies are very small, the contribution to the free energy change from van der Waals terms is negligible.

In Step 4, the charges of the hydrophobic complex X'Y' are gradually restored to their original values to yield the complex XY.

Steps 1 and 2 are shown in *Figure 2* as taking place in a single step with a free energy difference $\Delta G_1 = -\Delta G_{elec}(X) - \Delta G_{elec}(Y)$, but in practice, separate calculations are performed to obtain $-\Delta G_{elec}(X)$ and $-\Delta G_{elec}(Y)$. ΔG_2 in *Figure 2* corresponds to the

hydrophobic free energy change $\Delta G_2 = \Delta G_{hphobic} = \gamma(S_{X'Y'} - S_{X'} - S_{Y'})$. ΔG_3 in *Figure 3* corresponds to $\Delta G_{elec}(XY)$, the step that completes the thermodynamic cycle.

The charging and uncharging free energies (ΔG_{elec}) are calculated using slow-growth thermodynamic integration. In these slow-growth simulations, the system is gradually transformed from state *r* (reactants) to state *p* (products) by incrementally changing a coupling parameter λ from 0 to 1 over the course of a MD simulation, and the free energy difference ΔG_{pr} is obtained by evaluating the integrodifferential equation:

$$\Delta G_{pr} = G_p - G_r = \int_0^1 d\lambda(\partial G/\partial\lambda) = \int_0^1 d\lambda \left\langle U_p(\Omega) - U_r(\Omega) \right\rangle_\lambda \quad [7]$$

where $U_r(\Omega)$ and $U_p(\Omega)$ are the potential energy functions of states *r* and *p*, respectively, Ω represents the entire set of coordinates used to describe the system, and $\langle\theta\rangle$ enotes an ensemble average of θ on potential surface $U(\Omega, \lambda)$, which is specified by the relation:

$$U(\Omega,\lambda) = U(\Omega) + \lambda\left[U_p(\Omega) - U_r(\Omega)\right] \quad [8]$$

Steps 1, 2, and 4 in the above reaction scheme each entail the performance of slow-growth calculations in separate systems. Sulfonamide+water systems typically contain about 390 water molecules, while the βCD+water and sulfonamide/βCD+water systems contain about 460 water molecules.

Before a given slow-growth calculation is initiated, each system is taken through the following four-step annealing process: a 15 psec simulation during which the temperature is raised (linearly) from 0 K to 500 K, followed by 5 psec at 500 K, followed by 10 psec during which the temperature is lowered from 500 K to 300 K, followed by 5 psec at 300 K. This annealing procedure allows each system to escape from local potential energy minima and to find more favorable regions of configuration space. Slow-growth integration calculations are then carried out over 40 psec simulations at 300 K. The reproducibility of slow-growth free energy calculations is usually checked by performing both "forward" and "backward" calculations, where "forward" means evaluating Eq. 2 as it is written, and "backward" means exchanging the limits of integration in Eq. 2. The amount of CPU time required for Method 1 calculations made it unfeasible to perform more than one slow-growth integration for each electrostatic free energy. However, based on forward and backward integrations performed on smaller systems, the error range for electrostatic free energies of uncharged solute species is about 0.5 kcal/mol with this methodology.

Additional calculations are not needed to obtain the hydrophobic free energies, $\Delta G_{hphobic}$. This is because the average solvent-accessible surface areas $S_{X'Y'}$, $S_{X'}$, and $S_{Y'}$ may all be calculated during the electrostatic free energy calculations of the relevant systems.

RESULTS AND DISCUSSION

NMR Spectroscopy

Results of the NMR studies are listed in *Tables I and II*. It was thought at first that the preferred conformations could be ascertained from the NMR spectra by examining which of the sulfonamide protons were shifting upfield. However, as *Table II* shows, this means of determining which of the two rings is in the βCD cavity is ambiguous. *Table II* lists the chemical shift and linewidth changes in the proton spectra of the sulfonamides due to complexation with βCD. It is obvious that although the sulfonamide proton resonance frequencies shift in the bound state relative to the free state, there is no consistent upfield or downfield trend in these shifts which would allow us to determine which end of the molecules are inside the βCD cavity. We note, however, that there is clear evidence in the data (*Table II*) that only the protons of one ring undergo significant line broadening upon complexation. *Figure 3* illustrates the line broadening effect of βCD on the aniline ring resonances of sulfathiazole (compound 4). In the figure we observe that the aniline ring resonances shift upfield and broaden by 50% (2.0 Hz to 3.0 Hz) in the complexed state (*Fig. 3B*). However, the thiazole ring protons shift

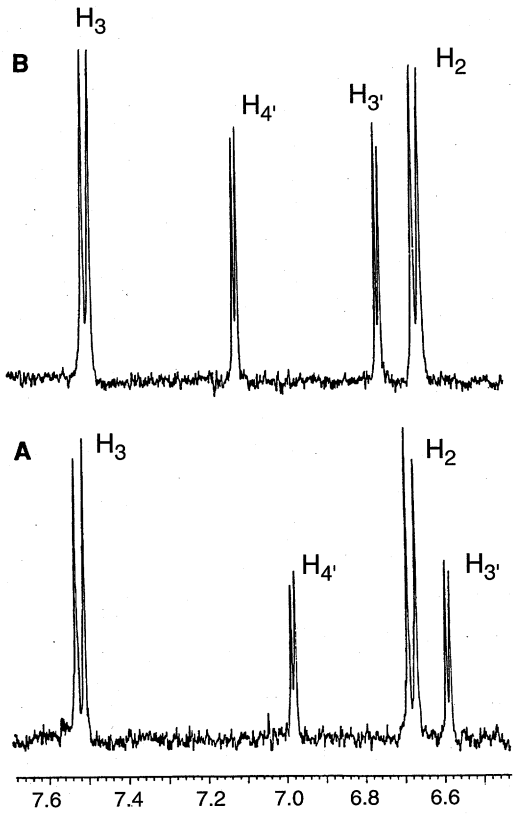

FIGURE 3. 400 MHz 1H spectra of A) saturated solution (roughly 0.8 mg/ml) of sulfathiazole in D_2O; B) same solution as A, but containing an equal molar amount of βCD. Each spectrum was obtained with 16 scans, a pulse delay of 45 sec, spectral width of 4000 Hz, 16K data points, and a 90° pulse of 8.0 μsec.

Sulfonamide	Method 1*	Method 2†	Solubility§	HPLC‡	^{1}H NMR¶
sulfathiazole	**-21.1**	**-18.3**	-4.44	-4.46	-4.45±0.02
	-14.9	-17.4			
sulfamethizole	-16.8	**-18.5**	-4.13	-4.23	—
	-18.8	-18.3			
sulfadiazine	-19.8	**-17.9**	-3.45	-3.45	-3.44±0.07
	-21.8	-15.7			
sulfamerazine	**-18.1**	-21.3	-2.97	-3.19	-3.07±0.06
	-16.1	-21.3			
sulfamethazine	**-14.9**	**-21.1**	—	—	-2.97±0.14
	-13.1	-14.4			
sulfisomidine	**-20.2**	**-18.3**	-2.88	-2.93	—
	-17.9	-14.2			

* Model system contains solvent.
† Model system does not contain solvent.
§ Ref. 4.
‡ Ref. 5.
¶ Determined in 20 mM phosphate buffer (pre-exchanged with D_2O), pH=7, 25°C. All free energy values are given in kcal/mol. In the Method 1 and Method 2 columns, the first of the two rows corresponds to the complex conformation with the aniline ring inserted into the βCD cavity, and the second row corresponds to the conformation with the variable ring inserted. The conformation with the lower free energy (the apparent preferred conformation) is indicated with boldface type.

downfield in the complexed state without any appreciable broadening. This line broadening effect is a consequence of the slowed motion and dipolar interactions of the embedded ring protons in the cavity (14). T_2 values reflect the same trend (data not shown).

Thus, compounds 1 and 4 interact with βCD through their aniline rings, whereas compounds 2 and 3 appear to bind with their respective pyrimidine rings within the cavity. A previous study (15) utilizing ^{13}C T_1 values suggested that sulfathiazole binds to βCD through its aniline ring. However, in the present study such a conclusion was not clear cut, since all of sulfathiazole's carbon resonances underwent a shortening of T_1 upon complexation.

In *Figure 4* Job's method of continuous variation (8) (see Experimental section) is used to illustrate that the stoichiometry of the sulfadiazine/βCD complex is 1:1. Based upon the size and shape similarities of the series of sulfonamides we included in this study, the stoichiometries of the other sulfonamide/βCD complexes were also assumed to be 1:1.

The association constants obtained from our ^{1}H NMR studies for compounds 1, 2, 3, and 4, are 151±35, 180±18, 334±40, and 1850±61 respectively. The results for 2, 3, and 4 are in excellent agreement with the association constants determined in solubility (4) and HPLC (5) studies. An association constant was not reported for compound 1 in Refs.4 and 5.

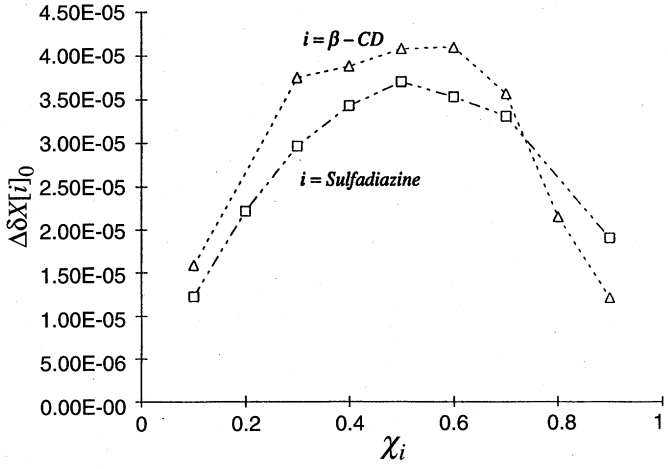

FIGURE 4. Job's method of continuous variation applied to the sulfadiazine/βCD inclusion complex. The maxima of both curves occurring at mole fraction 0.5 is indicative of 1:1 stoichiometry.

Calculations

The six sulfonamides examined in the computational portion of this study are illustrated in *Figure 1*. The four sulfonamides examined in the ^{1}H NMR portion of this study are designated in *Figure 1* as compounds 1, 2, 3, and 4, and their non-exchanging protons have been labeled for reference to the NMR spectral peaks (*Table II*). The results of the calculations are summarized in *Tables I, III* and *IV*. In *Table I*, the relative association free energies of the six sulfonamide/βCD complexes calculated using the two dif-

TABLE II

Chemical shifts of sulfonamide protons, and changes in chemical shifts upon complexation

	$\delta_H$free*					$\Delta\delta_H$bound†				
Compound	H_2	H_3	$H_{3'}$	$H_{4'}$	Me	H_2	H_3	$H_{3'}$	$H_{4'}$	Me
1 Sulfamethazine	7.60	6.80	-	6.63	2.32	0.02	-0.14	-	0.04	0.05
	(1.4)§	(1.3)	-	(2.2)	(2.2)	(3.1)	(3.0)	-	(3.0)	(2.6)
2 Sulfamerazine	7.68	6.80	8.13	6.76	2.34	0.02	-0.10	0.09	0.07	0.03
	(3.2)	(3.0)	(3.2)	(3.5)	(2.4)	(2.8)	(2.9)	(5.2)	(4.9)	(2.8)
3 Sulfadiazine	7.62	6.75	8.27	6.83	-	0.02	-0.08	0.05	0.06	-
	(3.0)	(2.8)	(3.9)	(3.6)	-	(3.3)	(3.2)	(6.0)	(6.3)	-
4 Sulfathiazole	6.66	7.50	6.56	6.96	-	-0.05	-0.17	0.02	0.05	-
	(2.0)	(2.0)	(2.0)	(2.0)	-	(3.0)	(3.0)	(2.0)	(2.0)	-

* ppm in D_2O containing 20 mM phosphate, pH = 7.0.

† 3.6:1 ratio (CD:sulfonamide, negative $\Delta\delta_H$ values indicate an upfield shift.

§ Values within parentheses, ( ), are full linewidths at half peak height in Hz.

ferent model systems (Methods 1 and 2) are reported. Association free energies obtained from solubility studies (4), HPLC studies (5), and our ^{1}H NMR studies are also given. (In the last three columns, standard association free energies, $\Delta G°$, were obtained from the corresponding association constants, K_a, with the relation $\Delta G° = -RT ln K_a$, where *R* is the ideal gas constant and *T* is the absolute temperature.) The Method 1 and Method 2 columns each have two rows of data. The first of the two rows corresponds to the complex conformation with the aniline ring inserted into the βCD cavity, and the second row corresponds to the conformation with the variable end inserted into the βCD cavity.

All calculated free energies are relative, rather than standard, since the solute species in the model systems are not in their standard states, and correcting to standard state concentrations is not straightforward (the volumes of the systems are not well-defined quantities). The differences between free energy values within a given column of the table, however, should be comparable to the differences in adjacent columns.

The first test of the two computational methods is whether they produce the six association free energies in the same order as the corresponding experimental values. As can be seen from *Table I*, neither Method 1 nor Method 2 was able to satisfy this test. It is of interest to note, however, that by shifting each of the Method 1 values up or down by 0 to 1.5 kcal/mol, the proper order can be obtained. This means that the error range associated with Method 1 may be as small as, but is probably not less than ± 1.5 kcal/mol. (Note: this is not a definitive estimate of the error bars associated with these calculations. The error bars of free energy calculations are notoriously difficult to obtain. More well-defined estimates of the errors could be obtained if each calculation were repeated a number of times, as is done for normal laboratory experiments, from which average values and deviations from the averages may be obtained. The amount of time these additional calculations would have required, prevented us from attempting this.) Method 1 in its current form is therefore not useful if one needs to discriminate amongst association free energies that differ by less than 1.5 kcal/mol, as is the case in this study. A better test of the computational methods would have been to examine a set of reference complexes having a wider range of association free energies.

Least-squares straight line fits of the calculated free energies to the experimental values yield basic trends in the calculated results.The least-squares fit for Method 1 results is: $\Delta G_{expt} = 2.56(\Delta G_{calc,1} + 18.6)$, and the fit for Method 2 results is: $(G_{expt} = -1.59(\Delta G_{calc,2} + 21.1)$. The correlation coefficients are 0.171 and 0.307 for Methods 1 and 2, respectively, neither of which is very good. We expected to obtain fits of the form $\Delta G_{expt} = a_1(\Delta G_{calc} + a_0)$ with the coefficient a_1 close to unity. The negative correlation between ΔG_{expt} and $\Delta G_{calc,2}$ values warns against the use of Method 2 in any future work.

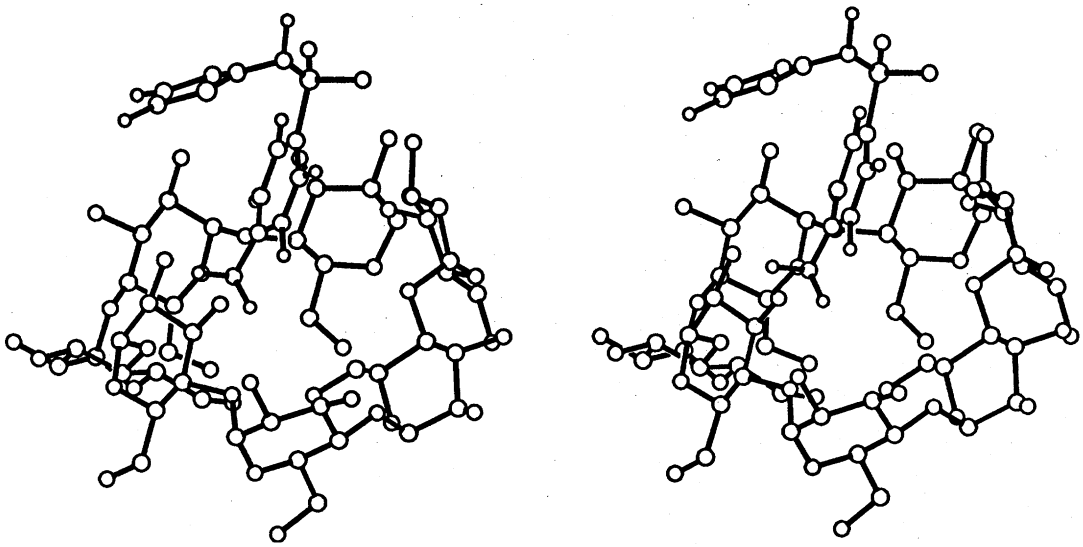

FIGURE 5. Stereo view of a ball-and-stick representation of the sulfathiazole/βCD inclusion complex, in its preferred conformation with the aniline ring inserted within the βCD cavity. Water molecules are not shown, nor are the βCD hydrogen atoms. (stereo viewing glasses are recommended for examining this figure)

TABLE III
Prediction of binding conformations by methods 1 and 2

Sulfonamide	Method 1	Method 2	NMR
sulfathiazole	Ring R*	Ring R	Ring R
sulfadiazine	Ring R'	Ring R	Ring R'
sulfamerazine	Ring R	Toss up	Ring R'
sulfamethazine	Ring R	Ring R	Ring R

* Ring R indicates that the conformation with the aniline ring inserted into the βCD cavity is the apparent preferred conformation, while Ring R' indicates that the conformation with the variable ring inserted is preferred. Method 1 agrees with the NMR results in three out of the four cases, while Method 2 agrees with the NMR results in two or three out of the four cases.

TABLE IV
Breakdown of electrostatic and hydrophobic association free energy differences (method 1)

Sulfonamide	ΔG_{elec}*	$\gamma(S_{X'Y'} - S_{X'} - S_{Y'})$
sulfathiazole	-1.6	-19.5
	-0.8	-14.1
sulfamethizole	+2.1	-18.9
	+3.0	-21.8
sulfadiazine	-2.2	-17.6
	-2.0	-19.8
sulfamerazine	-1.7	-16.4
	-0.3	-15.8
sulfamethazine	+4.6	-19.5
	+5.7	-18.8
sulfisomidine	-1.8	-18.4
	+1.0	-18.9

* Energies are expressed in kcal/mol. As in *Table I*, the first of the two rows corresponds to the complex with the aniline ring inserted into the βCD cavity, and the second row corresponds to the complex with the variable ring inserted. $\Delta G_{elec} = \Delta G_{elec}(XY) - \Delta G_{elec}(X) - \Delta G_{elec}(Y)$. $\gamma = 0.050$ kcal mol^{-1} Å^{-2} is the microscopic surface tension, and S_A is the average solvent-accessible surface area of solute species A.

The second test of the computational methods is whether they correctly select the preferred conformation of each sulfonamide/βCD complex. Calculations were performed for both of the two possible conformations. The conformation that yielded the lower free energy was taken as the preferred conformation. The actual preferred conformations of four of the six complexes were determined in our ^{1}H NMR studies (the other two compounds were not available at the time of this study). A comparison of the predicted and actual preferred conformations is given in *Table III*. Entries designated as Ring *R* indicate that the preferred conformation is the one with the aniline ring inserted within the βCD cavity, while entries designated as Ring *R'* indicate that the conformation with the variable ring inserted is the preferred one. Method 1 selects the correct conformation in three out of the four cases, and is thus fairly reliable in determining the more stable of two conformations. In the Method 2 calculation for the sulfamerazine/βCD complex, nearly identical association free energies were obtained for the two conformations, so a preferred conformation based upon a lower free energy could not be predicted. Thus, Method 2 selects the correct conformation in either two or three out of the four cases.

Method 2 calculations are quite fast compared to those of Method 1. Each Method 2 value reported in the table was obtained in only a few CPU hours on an Iris 4D/35 workstation (6). In Method 1, the solvated sulfonamide systems are typically 14 Å in radius and contain about 390 water molecules. The solvated CD and sulfonamide/CD systems are typically 15.5 Å in radius and contain about 460 water molecules. Method 1 calculations typically require 250 CPU hours to obtain a single association free energy value.

Although the 1.5 kcal/mol error range for Method 1 calculations put hopes of reproducing the association energies of the six reference complexes out of reach, the results of the calculations still provide some interesting insights. A decomposition of Method 1 association free energies into electrostatic and hydrophobic contributions is presented in *Table III*. If sulfonamide/βCD complex formation was driven solely by the hydrophobic effect (*i.e.* the tendency of water to "corral" nonpolar solutes), all of the electrostatic free energies — the essentially enthalpic portion of the free energies — would be greater than zero. This, however, is not the case. The fact that electrostatic free energies are negative in four out of the six systems examined indicates that the binding of sulfonamides (and perhaps other types of guest molecule) to CD should not be thought of as a purely hydrophobic phenomenon. The idea that guest/CD inclusion complexation is not due purely to solute hydrophobicity can also be inferred from a recent study (16) in which both ΔH and ΔS were found to be negative for the formation of the fenoprofen/βCD complex.

It is interesting to examine the geometries of the sulfonamide/βCD complexes after they have been allowed to relax via molecular dynamics simulations of the Method 1 model. *Figure 5* displays a ball-and-stick stereo view of the sulfathiazole/bCD complex in its preferred conformation with the aniline ring inserted into the βCD cavity (stereo viewing glasses are recommended for examining this figure). The water present in this system is not shown in the figure, nor are the βCD hydrogen atoms. This sulfathiazole/βCD structure is typical of the complexes we studied. From the figure we see that the term "inserted" is a relative one, since the βCD molecule adopts a structure which is more open than structures obtained from gas phase methods such as Method 2. There is, therefore, less of a cavity for the sulfonamide to bind to. The "lock-and-key" effect exhibited by many ligand-receptor complexes is not at work here.

CONCLUSIONS

Although hydrogen bonds and other attractive electrostatic interactions exist between sulfathiazole and βCD, these interactions are not strong enough to immobilize sulfathiazole within the cavity. The molecular dynamics (MD) simulations show that the sulfonamides are still fairly labile even when bound. This finding is verified by our ^{1}H NMR studies (*Table II*), in which it was found that the linewidth T_2s (data not shown) of the protons of the ring not in the cavity did not change appreciably upon complexation to βCD. The computational methods used in this work may be described as semi-quantitative and relatively inconclusive. Further work is required to improve the methodology to the point where more quantitatively trustworthy results may be obtained. The fact that the association free energies obtained with Method 2 calculations possess a negative correlation with the experimental values as obtained from least-squares regression analysis should serve as a strong warning against the use of such *in vacuo* methods for the study of systems in which the solvent plays such an important role.

REFERENCES

1. Szejtli J. Cyclodextrin Technology, Chapter 2 Cyclodextrin inclusion complexes. Kluwer Academic Publishers, The Netherlands 1989; p. 79-185.
2. Dailey OD Jr, Bland JM, Trask-Morrell B. Preparation and characterization of cyclodextrin complexes of the insecticides Aldicarb and Sulprofos. *J Agric Food Chem* 1993; **41**:1767-71.
3. Pfeffer PE, Osman SF, Hotchkiss A, Bhagwat AA, Keister DL, Valentine KM. Cyclolaminarinose. A new biologically active β1,3 cyclic glucan. *Carbohydrate Research* 1997; **665**:23-37.
4. Cohen J, Lach JL. Interactions of pharmaceuticals with Schardinger dextrins. *J Pharm Sci* 1963; **52**:132.
5. Uekama K, Hirayama Fnasu S, Matsuo N, Irie T. Determination of stability constants for inclusion complexes of cyclodextrins with various drug molecules by high performance liquid chromatography. *Chem Pharm Bull* 1978; **26**:3477-84.
6. Mention of brand or firm name does not constitute an endorsement by the USDA over other products of a similar nature.
7. Meiboom S, Gill D. Measuring nuclear relaxation times. *Rev Sci Instrument* 1958; **29**:688-95.
8. Job P. Formation and stability of inorganic complexes in solution. *Liebigs Ann Chem* 1928; **9**:113.
9. (a) Gasteiger J, Marsili M. Iterative partial equalization of orbital electonegativity- A rapid access to atomic charges. *Tetrahedron* 1980; **36**:3219 (b) Marsili M, Gasteiger J. *Croat Chem Acta* 1980; **53**:601.
10. Dewar MJS, Thiel W. The MNDO method. Approximations and parameters. *J Am Chem Soc* 1977; **99**:4899.
11. King G, Warshel A. A surface constrained all-atom solvent model for effective simulations of polar solutions. *J Chem Phys* 1989; **91**:3647.
12. Clark M, Cramer III RD, Van Opdenbosch N. *J Comp Chem* 1989; **10**:982.
13. Nicholls A, Sharp KA, Honig B. Protein folding and association: insights from the interfacial and thermodynamic properties of hydrocarbons. *Proteins* 1991; **11**:281.
14. Shaw D. Fourier Transform NMR Spectroscopy; Elsevier, New York, 1976.
15. Uekama K, Hirayama F, Koinuma H. Carbon 13 spin-lattice relaxation times of the inclusion complex of β-cyclodextrin with sulfathiazole in aqueous solution. *Chem Lett* 1977; 1393-6.
16. Uccello-Barretta G, Chiavacci C, Bertucci C, Salvadori P. Stereochemistry and dynamics of the inclusion complex of (S)-(+)-fenoprofen with cyclomaltoheptaose (βcyclodextrin) *Carbohydrate Research* 1993; **243**:1-10.